tvst

https://doi.org/10.1167/tvst.8.4.1

Article

Avian Adeno-Associated Viral Transduction of the Postembryonic Chicken Retina

Derek M. Waldner[1], Frank Visser[2], Andy J. Fischer[3], N. Torben Bech-Hansen[4], and William K. Stell[5]

[1] Graduate Department of Neuroscience, Cumming School of Medicine, University of Calgary, Calgary, Alberta, Canada
[2] Department of Physiology and Pharmacology, Hotchkiss Brain Institute, University of Calgary, Calgary, Alberta, Canada
[3] Department of Neuroscience, The Ohio State University Wexner Medical Center, Columbus, OH, USA
[4] Department of Medical Genetics, and Department of Surgery, Alberta Children's Hospital Research Institute, and Hotchkiss Brain Institute, Cumming School of Medicine, University of Calgary, Calgary, Alberta, Canada
[5] Department of Cell Biology and Anatomy and Department of Surgery, Hotchkiss Brain Institute, and Alberta Children's Hospital Research Institute, Cumming School of Medicine, University of Calgary, Calgary, Alberta, Canada

Correspondence: Derek M. Waldner, Graduate Department of Neuroscience, Cumming School of Medicine, University of Calgary, 3330 Hospital Drive, Calgary, Alberta AB T2N4N1, Canada. e-mail: Derek.waldner@ucalgary.ca

Received: 19 February 2019
Accepted: 9 May 2019
Published: 1 July 2019

Keywords: AAV; avian; photoreceptor transduction

Citation: Waldner DM, Visser F, Fischer AJ, Bech-Hansen NT, Stell WK. Avian adeno-associated viral transduction of the postembryonic chicken retina. Trans Vis Sci Tech. 2019;8(4):1, https://doi.org/10.1167/tvst.8.4.1

Copyright 2019 The Authors

Purpose: The posthatching chicken is a valuable animal model for research, but molecular tools needed for altering its gene expression are not yet available. Our purpose here was to adapt the adeno-associated viral (AAV) vector method, used widely in mammalian studies, for use in investigations of the chicken retina. We hypothesized that the recently characterized avian AAV (A3V) vector could effectively transduce chick retinal cells for manipulation of gene expression, after intravitreal or subretinal injection.

Methods: A3V encoding enhanced green fluorescent protein (EGFP) was injected intravitreally or subretinally into P1-3 chick eye and left for 7 to 10 days. Retinas were then sectioned or flat-mounted and visualized via laser-scanning confocal microscopy for analysis of expression and imaging of retinal cells.

Results: Intravitreal A3V-EGFP injection resulted in EGFP expression in a small percent of retinal cells, primarily those with processes and/or cell bodies near the vitreal surface. In contrast, subretinal injection of A3V-EGFP within confined retinal "blebs" produced high rates of transduction of rods and all types of cones. Some examples of all other major retinal cell types, including horizontal, amacrine, bipolar, ganglion, and Müller cells, were also transduced, although with much lower frequency than photoreceptors.

Conclusions: A3V is a promising tool for investigating chick retinal cells and circuitry in situ. This novel vector can be used for studies in which local photoreceptor transduction is sufficient for meaningful observations.

Translational Relevance: With this vector, the postembryonic chick retina can now be used for preclinical trials of gene therapy for prevention and treatment of human retinal disease.

Introduction

Mice have historically been the most widely used animal models for research into human genetic disorders for many reasons, including anatomical, physiological, and genetic similarities to humans; small size; short generation time; cost efficiency; and availability of many tools for genetic manipulation.[1] For studies of human ocular disease, however, mice may not be optimal. In mice, visual spatial resolution is exceedingly low (equivalent to 20/2000 vision), the eyes and visual pathways are up to 100-fold smaller than those of primate models, and the retinas are rod-dominant; the last of these renders them poor candidates for studies of cone-afflicting human conditions, such as age-related macular degeneration and primary cone dystrophies.[2] As an alternative, the

This work is licensed under a Creative Commons Attribution-NonCommercial-NoDerivatives 4.0 International License.

postembryonic chick offers many advantages for ocular research, including relatively large eye size (leading to increased ease of ocular manipulations and measurements), cone-dominated retinas having high visual acuity, and precocial retinal development.[3] These and other characteristics make the chick an excellent model for visual research. Unfortunately, few tools exist for genetic manipulation of these animals, causing the majority of functional manipulations to rely on pharmacology.

Viral vectors are among the most versatile tools available for the manipulation of gene expression. The generation of transgenic animals can be expensive and time-consuming and in many cases can require several generations of breeding to derive the appropriate genotype for experimentation.[4,5] In contrast, properly designed viral vectors can be used to alter gene expression in a single generation, with temporal and spatial control determined by the time, quantity, and place of application.[6] There have been several published attempts to manipulate chick retinal gene expression by using a variety of vectors, all of which have been applied to embryos in ovo. Lentiviral vectors expressing retinal guanylate cyclase-1 have been used to rescue function and prevent degeneration in a chick model of Leber congenital amaurosis; but they transduced only 6% to 12% of retinal cells after injection into the neural tube at embryonic day 2, and expression was seemingly transient.[7,8] Additionally, replication-competent avian sarcoma-leukosis virus long terminal repeat with a splice acceptor (RCAS) viral vectors have been used in multiple studies for the delivery of transgenes to the embryonic chick retina, including interfering RNAs that successfully knocked down target mitochondrial RNAs.[9,10] Nonviral methods, including electroporation and sonication of naked DNA vectors, have also been successfully used to transduce early developing retinas in ovo and in culture.[9,11] None of these established methods, however, allows for sustained alteration of gene expression in the postembryonic chicken retina.

Adeno-associated viruses (AAVs) have recently become the most widely used viral vectors for the manipulation of retinal gene expression in nonavian animal models because of certain attractive features that are characteristic of them. AAVs are not known to cause disease, have broad tissue tropism, are minimally immunogenic, cannot replicate in the absence of helper virus coinfection, and can achieve efficient, long-lasting gene transfer.[12] Accordingly, AAVs are currently being tested in over 150 clinical trials worldwide as vectors for human gene therapy.[13] A number of different AAV serotypes have been isolated and characterized, which exhibit different tissue-, cell-, and species-specific transduction patterns.[14] For retinal research purposes, certain AAV serotypes have allowed scientists to transduce more than 30% of mouse photoreceptors following a single injection into the vitreous of the eye, creating an invaluable tool for studying retinal function and disease in mice.[15]

An avian homologue of known AAVs of nonhuman primates and other mammals was first identified in 1973, and the subsequent production of recombinants of this avian AAV (avian-AAV, or A3V) was achieved in 2003, allowing for the use of the vector for manipulation of gene expression in postmitotic avian cells.[16,17] In 2012, Matsui et al.[18] showed that injection of A3V resulted in highly efficient transduction of neurons in the posthatching chick brain in vivo, with a higher transduction rate than lenti- or mammalian AAVs. Thus, A3V may provide the first means of efficacious, reproducible manipulation of retinal gene expression in postembryonic, normally seeing and behaving chickens, making this increasingly powerful model for visual research even more attractive and useful. In this paper, we report our progress in producing and applying A3V as a vector for manipulating gene expression in postmitotic cells of postembryonic chicken retinas. Some of these findings were presented previously in a preliminary report.[19]

Materials and Methods

Animal Care and Ethics

Chicks were maintained in the University of Calgary Health Sciences Resource Centre (HSARC) under a 12:12 hour light-dark cycle. All experiments were approved by the Health Sciences Animal Care Committee of the University of Calgary under protocol AC14-0134 and were carried out in accordance with the Council on Animal Care Guide to the Care and Use of Experimental Animals and the Association for Research in Vision and Ophthalmology Statement for the Use of Animals in Ophthalmic and Vision Research. White Leghorn cockerels (*Gallus gallus domesticus*) of Shaver or Dekalb strain and broiler chicks of both sexes were purchased from Rochester Hatchery (Westlock, Alberta, Canada) and delivered on posthatching day one (P1).

Generation of Recombinant A3V Vectors

Avian-AAV vectors were generated and purified via the triple-plasmid transfection method and subsequent iodixanol gradient ultracentrifugation, modified from Zolotukhin et al.[20] and Reid and Lipinski.[21]

A3V Plasmid Constructs

The A3V-RepCap (A3V-RC) plasmid expressing A3V-specific replication and capsid proteins was kindly provided by Dr. J. Chiorini (National Institute of Dental and Craniofacial Research, National Institutes of Health).[16] pHelper was obtained from Agilent Technologies (Santa Clarita, CA) as a part of the AAV Helper-Free System (Agilent catalog no. 240071). To build the A3V-CAG-enhanced green fluorescent protein (EGFP) transfer vector, A3V-Rous Sarcoma Virus (RSV)-EGFP (a kind gift of Dr. R. Matsui and Dr. D. Watanabe, Kyoto University, Kyoto, Japan[18]) was restriction-digested with BglII and NcoI, releasing the RSV promoter and assembled using the NEBuilder Hifi DNA Assembly Kit (catalog no. E5520S; New England BioLabs [NEB], Ipswich, MA) with a CAG-containing fragment cloned from pCAG-DsRed (Addgene plasmid no. 11151).[22] The following primers (containing necessary homologous sequence for assembly into open A3V-EGFP backbone and CAG-specific amplification sequence) were used: F' CAG Insert, 5′-CCGGTGAGGTAATGCCGTCACGTGAGATCTGCGTTACATAACTTACGGTAAATG-3′; and R' CAG Insert, 5′-TGAACAGCTCCTCGCCCTTGCTCACCATGGGAAGGCAACGCAGCGACTC-3′. The resulting vector (A3V-CAG-EGFP) features a CAG-EGFP-WPRE-SV40-pA cassette flanked by A3V-specific inverted terminal repeats (ITRs) necessary for encapsulation into A3V virions by A3V-specific replication and capsid proteins. This transfer plasmid was used to generate all A3V virions used in these experiments.

All plasmids were transformed into competent *Escherichia coli* cells (NEB 5-alpha or DH5alpha) for amplification. Transformed *E. coli* cells were grown in 250 mL Luria broth cultures containing appropriate selection antibiotics (ampicillin for A3V-RSV-EGFP, A3V-CAG-EGFP, and pHelper; kanamycin for A3V-RC), after which plasmid DNA was isolated and purified using the NucleoBond Xtra Maxi Plus kit according to the manufacturer's instructions (catalog no. 740416.50; Macherey-Nagel, Düren, Germany). All vectors were verified by restriction digest and/or DNA sequencing.

Triple Plasmid Transfection

Human embryonic kidney 293T (HEK293T; catalog no. R70007; ThermoFisher, Waltham, MA) cells were grown at 37°C and 5% CO_2 in "complete" medium (Dulbecco's modified Eagle's medium [high glucose, pyruvate; catalog no. 1995065; ThermoFisher] supplemented with 10% fetal bovine serum [catalog no. 12483020; ThermoFisher], 50 U/mL penicillin-streptomycin [catalog no. 15070063; ThermoFisher], and 1× Minimum Essential Medium Non-Essential Amino Acids [catalog no. 11140050; ThermoFisher]) in either 10× 15-cm petri dishes or 1 Corning HYPERflask cell culture vessel. Upon reaching ~80% confluency, cells were transfected via calcium phosphate or polyethylenimine (PEI) co-transfection methods. Calcium phosphate cotransfection was performed as described for lentiviral production, with plasmid concentrations adjusted as needed (Dr. Didier Trono, https://tronolab.epfl.ch/page-148635-en.html). PEI cotransfection was performed as described by Reid and Lipinski[21] using a 1-mg/mL PEI solution. Both methods used equimolar concentrations of pHelper, A3V-RC, and transfer plasmid (A3V-CAG-EGFP) in 500-µg total DNA per preparation. Transfected cells were incubated for 72 hours before proceeding.

HEK293T Cell Lysis

After the 72-hour incubation period, transfected cells were detached by scraping (petri dishes) or vigorous shaking (HYPERflask) and pelleted by centrifugation at 400 g for 15 minutes. The A3V-containing cells were then resuspended in 15 mL lysis buffer (150 mM NaCl and 50 mM Tris–HCl [pH 8.5]) and alternated between a dry-ice/ethanol mixture (~30 minutes/cycle) and 37°C water bath (until completely thawed) four times to lyse cells and release the A3V virions. Benzonase nuclease was then added to the lysate to a final concentration of 50 U/mL and incubated for 1 hour at 37°C to degrade cellular nucleic acids. Cellular debris was pelleted by centrifugation at 24,000 g for 20 minutes, and the "crude lysate" supernatant was carefully decanted.

Iodixanol Step-Gradient Ultracentrifugation

Iodixanol gradient layers of 15%, 25%, 40%, and 60% were prepared from OptiPrep Density Gradient Medium (catalog no. D1556; Sigma-Aldrich, St. Louis, MO) and 5× PBS-MK (685 mM NaCl, 26 mM KCl, 40 mM Na_2HPO_4, 10 mM KH_2PO_4, and 5 mM $MgCl_2$) to a final concentration of 1× phosphate buffered saline-magnesium potassium (PBS-MK), with phenol red included in the 25% and 60% layers

for gradient visualization and 1 M NaCl included in the 15% layer for disruption of ionic interactions between viral particles. Step-gradients were prepared in Beckman OptiSeal Ultracentrifuge tubes (catalog no. 361625; Beckman Coulter, Brea, CA) by underlaying iodixanol layers as described in Reid and Lipinski.[21] Iodixanol step-gradients were ultracentrifuged in a T70 Ti rotor at 59,000 RPM for 90 minutes at 18°C; then, ~4 mL of each gradient was aspirated from ~2 mm below the 40% to 60% interface and diluted in 100 mL sterile Hank's Balanced Salt Solution with 0.014% Tween-20. The diluted virus solution was concentrated in an Amicon Ultra-15 centrifugal filter unit (100 kDa MWCO; catalog no. UFC910008; EMD Millipore, Burlington, MA), according to the manufacturer's instructions, to a final volume of ~250 µL; this was followed by two washes with 10 mL Hank's Balanced Salt Solution/Tween-20 solution. Purified virus preps were concentrated to a final volume of ~200 µL, aliquoted, and frozen at −80°C for future quality-control and transduction experiments.

Sodium Dodecyl Sulfate-Polyacrylamide Gel Electrophoresis (SDS-PAGE), RT-PCR, and In Vitro Transduction

Capsid Protein Analysis

The purity of the A3V vectors was assessed via SDS-PAGE analysis. A total of 10 µL of purified vector was denatured in reducing sample buffer by incubation at 95°C for 5 minutes, followed by separation on a 9% SDS-PAGE polyacrylamide gel for 80 minutes at 140 V. Gels were stained with InstantBlue Ultrafast Protein Stain (catalog no. ISB1L-1L; Sigma-Aldrich) overnight to visualize capsid proteins.

Vector DNA Analysis

Vector DNA was quantified by real-time polymerase chain reaction (RT-PCR) analysis as described in Zolotukhin et al.,[20] with minor modifications. Briefly, 5 µL of purified virus was incubated for 1 hour at 37°C with 1 µL proteinase K, in a solution of 10 mM Tris-HCl, 10 mM EDTA, and 1% SDS [pH 8.0] in 20-µL final volume. This solution was then incubated at 98°C for 10 minutes to lyse viral particles further and, thus, release encapsulated genomes. The viral genome DNA was then isolated by silica membrane spin column purification, using the NucleoSpin Gel and PCR Clean-up system (catalog no. 740609.50; Macherey-Nagel), according to the manufacturer's instructions, with final elution into 25 µL. RT-PCR was performed on 1:100 diluted, 1:10 diluted, and undiluted viral eluates, using KAPA SYBR Fast Universal Kit (catalog no. KK4601; Sigma-Aldrich) following the manufacturer's instructions; a standard curve was established with 10^4 to 10^{13} copies/mL of a known GFP-expressing plasmid and the following primers (specific to EGFP): F': 5′-CACTACCAGCAGAACACCCC-3′ and R': 5′-GTCCATGCCGAGAGTGATCC-3′. Samples having standard curve and/or A3V cycle threshold values outside the linear range were eliminated from final titer calculations. Titer values (reported as genome copies/mL [GC/mL]), derived from the standard curve calculations, were adjusted to account for dilutions and expected loss during virion lysis and silica membrane purification (10-fold for 1:1 [undiluted] A3V, 100-fold for 1:10 A3V, and 1000-fold for 1:100 A3V). This quantification method reported A3V titers ranging from 10^{12} to 10^{13} GC/mL for all viral stocks produced.

In vitro verification of transduction was performed on primary cultures of chicken embryonic fibroblast (CEF) cells (a kind gift of Dr. Cairine Logan), maintained at 37°C and under 5% CO_2, in complete media (See above, Triple Plasmid Transfection) in 24-well plates. CEF cells were transduced with 10-µL serial dilutions of A3V as previously described, and finally GFP expression was visualized after 48 hours.[16]

A3V Intravitreal and Subretinal Injections

For both intravitreal and subretinal injections, P1-3 chicks were anesthetized with 1.5% isofluorane in O_2:N_2O (50:50); only the right eye was treated. Intravitreal injections were performed as previously described (Fig. 1).[23] Briefly, upper eyelids were cleaned externally with 70% ethanol, and injections were made using a 26-gauge needle on a 25-µL Hamilton Gastight syringe. The needle was inserted approximately 6 mm deep, through dorsal eyelid and sclera, and 20 µL containing 10^{12} to 10^{13} A3V GC/mL (10^{10}–10^{11} total genome copies) was injected rapidly into the vitreous. Subretinal injections were performed as described in Cebulla et al.[24] Briefly, lids were held open with a custom speculum, and Genteal gel was applied to the cornea. A 26-gauge bevelled needle was used to create a small hole in the temporal sclera, through which a 30-gauge blunt-tip needle was then used to deliver the subretinal injection. The needle was inserted and directed toward the central upper retina until a slight increase in resistance could be felt, indicating contact with the posterior aspect of

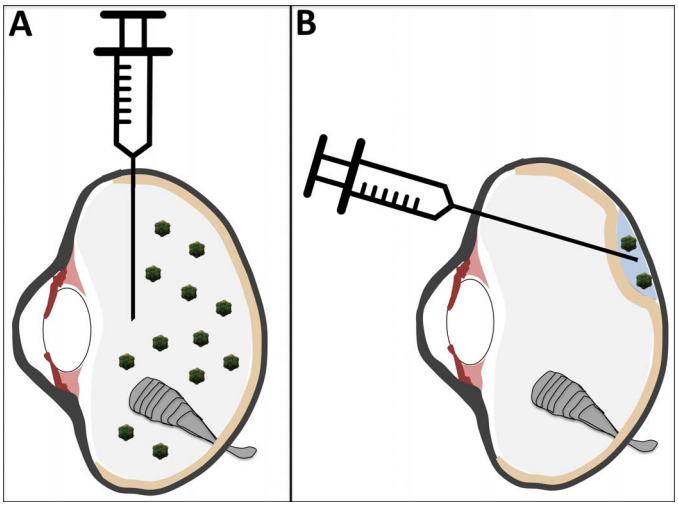

Figure 1. Methods of injection for transduction of the chicken retina. Schematic illustrating intravitreal (*left*) and subretinal (*right*) methods of A3V-injection into the chicken eye.

the globe. A total of 20 µL of 10^{12}- to 10^{12}-GC/mL A3V was then delivered by slowly depressing the plunger while maintaining this contact, with exceptional care taken to avoid applying excessive force and thereby to risk puncturing the globe. Erythromycin ophthalmic ointment was applied to the entry site after injection.

Tissue Preparation

Ten to 21 days after A3V delivery, chicks were euthanized by intraperitoneal injection of 0.2 mL Euthanyl (pentobarbital sodium, 240 mg/mL; CDMV, Saint-Hyacinthe, PQ, Canada), followed by decapitation. The injected eye was then enucleated and hemisected through the equator, and the vitreous was gently removed from the posterior segment. Posterior eye cups were then fixed in 4% paraformaldehyde + 3% sucrose in 0.1 M phosphate buffer (pH 7.4) for 45 to 60 minutes at room temperature (RT; ca. 20°C), then washed three times (15 minutes each) in PBS, and subsequently cryoprotected in 30% sucrose + 0.01% sodium azide for several days at 4°C. Retinal sections were prepared by mounting and freezing eyecups in Optimal Cutting Temperature (O.C.T.) compound, cryosectioning at 12 µm, and thaw-mounting onto Fisherbrand Superfrost Plus Microscope slides (catalog no. 4951PLUS4; ThermoFisher). Retinal whole mounts were prepared for immunolabeling by gently separating the retina and retinal pigment epithelium (RPE) from the posterior segment prior to fixation (cutting around the pecten for complete separation) and then mechanically separating the retina and RPE where necessary. Subsequent fixation was then performed as above.

Immunohistochemistry

Retinal sections on slides were washed in PBS to remove O.C.T. compound and incubated in 1:1000 rabbit anti-GFP antibody (catalog no. A-11122; ThermoFisher) in PBS + 0.3% Triton X-100 overnight at RT. Antibody labeling was detected the following day by washing in PBS (3 × 10 minutes), incubating for 2 hours in 1:500 Alexa Fluor 488-conjugated donkey anti-rabbit secondary antibody (catalog no. 711-545-152; Jackson ImmunoResearch Laboratories, Bar Harbor, ME), washing again in PBS (3 × 10 minutes), and mounting for observation in Fluoroshield with 4′,6-diamidino-2-phenylindole (DAPI) histology mounting medium (catalog no. F6057-20ML; Sigma-Aldrich). For labeling of retinal whole mounts, retinas were equilibrated in PBS, then immersed in 1:500 rabbit anti-GFP antibody in PBS + 0.3% Triton X-100 for 1 to 3 days, washed in PBS (3 × 20 minutes), and incubated in 1:500 Alexa Fluor 488-conjugated donkey anti-mouse secondary overnight at RT. Whole mounts were then extensively washed in PBS (3 × 30 minutes) and mounted on slides with Fluoroshield with DAPI, flanked by coverslip spacers to avoid damage from excessive flattening when applying the coverslip.

Microscopy and Digital Image Processing

Cross sections were viewed and images were captured on an Olympus FV1000 laser-scanning confocal microscope with a 60× objective (1.42 oil, PlanApoN), in the Snyder Institute (University of Calgary) Live Cell Imaging Facility as z-stacks at Nyquist resolution. Whole mounts were viewed and images were captured and stitched on an Olympus VS110-S5 Virtual Slide Scanner in the HBICore Advanced Microscopy Platform (AMP) facility. Digital image processing (including generation of z-stack projections) was performed with Image J 1.47. There is substantial variability in thickness across the chicken retina.[25] Therefore, for quantification of cell-specific transduction, DAPI-labeled retinal sections from the typical region of subretinal injection were analyzed to estimate approximate numbers of each cell type per millimeter of section, making the following assumptions for ease of analysis: (1) All cells in the outer nuclear layer (ONL) are photoreceptor cells[26]; (2) all cells in the distal inner nuclear layer (INL) monolayer in direct contact with the OPL

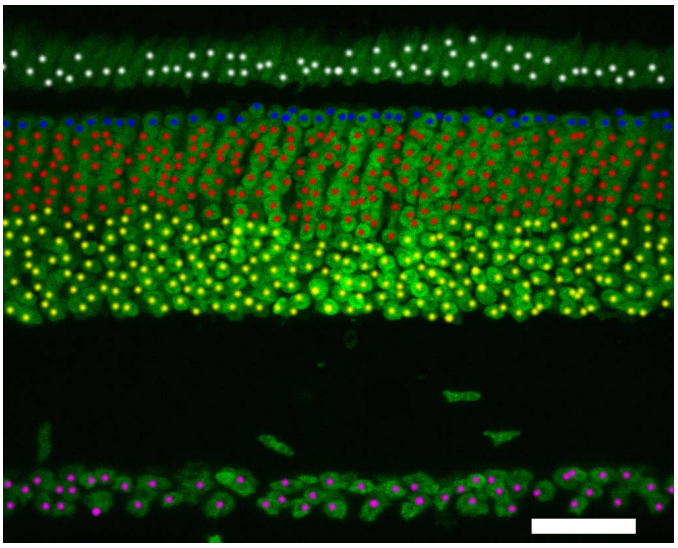

Figure 2. Representative counts of cells used to generate estimation of cell type per horizontal mm of chicken retinal sections. The 60× DAPI-labeled chicken retina used to estimate number of each cell type per horizontal millimeters of section, following assumptions described above (Microscopy and Digital Image Processing). *Colored dots* indicate cell types as follows: *white*, photoreceptors; *blue*, horizontal cells; *red*, bipolar cells; *yellow*, amacrine cells; and *purple*, ganglion cells. Scale bar = 25 μm.

are horizontal cells[27]; (3) Müller cell bodies form a monolayer in the INL and, therefore, have the same frequency as horizontal cells[28]; (4) cells in the distal 50% of the INL that are not horizontal cells are bipolar cells[29]; (5) cells in the proximal 50% of the INL are amacrine cells[29]; (6) Müller cell nuclei appear in the central INL and might be included in the counts of both distal and proximal halves of the INL and, therefore, one-half of the estimated number of Müller cells was subtracted from the counts of both amacrine and bipolar cells; (7) all cells in the granule cell layer (GCL) are ganglion cells. Displaced cells in the IPL were not counted. These assumptions for rough quantification disregard the known numbers of displaced amacrine cells in the GCL (reported to be ~13% of cells in GCL),[30] displaced ganglion cells in the IPL and INL,[31] and other factors. Figure 2 shows a representative image with cell identities assigned as described. This method led to the estimated cell-type counts shown below in the Table.

A total of 22 sections of eGFP-encoding A3V subretinally injected retinas were analyzed, counting the number of transduced cells of each type per millimeter of section (~35.5-mm transduced retina total). These values were divided by the estimated mean total number of cells/mm from Table to estimate the percent transduction of each retinal cell type in the chicken retina by A3V vectors.

Table. Approximate Quantification of Each Retinal Type in Typical Region of Subretinal Injection of Postembryonic Chicken Retina[a]

Cell Type	Mean % of Total ($n = 3$)	Standard Deviation, %	Mean Cells/mm ($n = 3$)	Standard Deviation
PRs	10.0	0.3	406	9
HCs	7.3	0.2	298	19
Bipolar	37.4	2.2	1524	83
Amacrine	29.9	2.6	1219	148
Müller	7.3	0.2	298	19
Ganglion	8.4	0.7	343	22
Total			4087	194

[a] n = 60× DAPI-labeled chick retina image, containing ~1400 cells.

PR, photoreceptors; HC, horizontal cells.

Results

Transduction of Inner Retinal Neurons following Intravitreal Injection

Intravitreal injection is the technically easiest, most direct, and noninvasive method of viral vector delivery to the retina and potentially allows for viral contact with the entire inner retinal surface. Additionally, intravitreal injection of some AAV serotypes has been sufficient for broad transduction of retinal cells in mammalian models.[15,32] Therefore, we first assessed the ability of A3V vectors to transduce the postembryonic chick retina via intravitreal delivery.

Figure 3 is a representative image showing the effects of a typical retinal transduction, as we observed in over 20 intravitreal injections of EGFP-encoding A3V vectors. No significant autofluorescence or anti-EGFP signal was observed in control or sham-injected retinas; therefore, all fluorescence was assumed to result from A3V-induced EGFP expression (Supplementary Fig. S1). These retinas exhibited meagre transduction, which was restricted almost exclusively to retinal ganglion (Fig. 3, black arrows) and Müller cells (Fig. 3, white arrows), although other cell types were occasionally observed (cell identities were verified by through-focus following of cell processes and/or higher resolution visualization). As EGFP expression is not confined to the cell bodies of

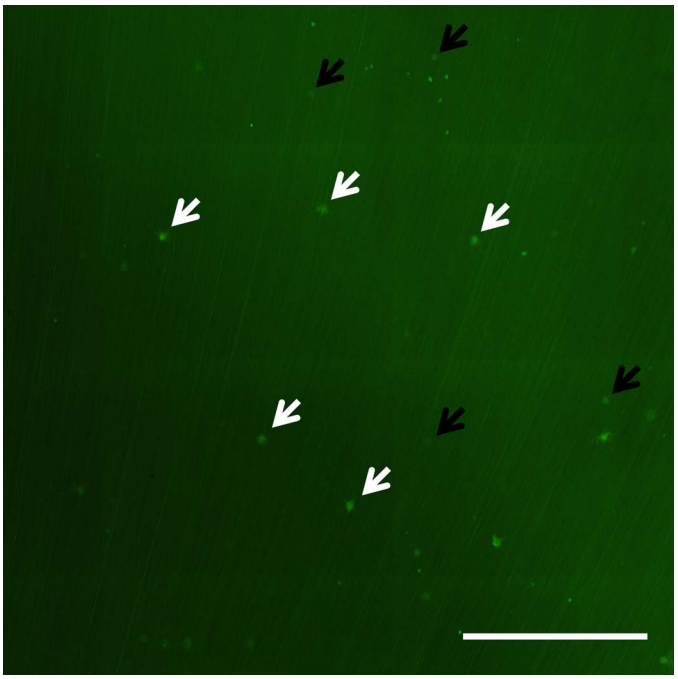

Figure 3. Transduction of inner retinal neurons with intravitreal injection of A3V. Representative 20× field of a whole-mounted chick retina 14 days following intravitreal delivery of EGFP-encoding A3V and anti-GFP immunolabeling as described above (Immunohistochemistry). *White arrows* indicate clusters of end feet of transduced Müller cells at the ILM; black arrows indicate transduced retinal ganglion cells. Scale bar = 500 μm.

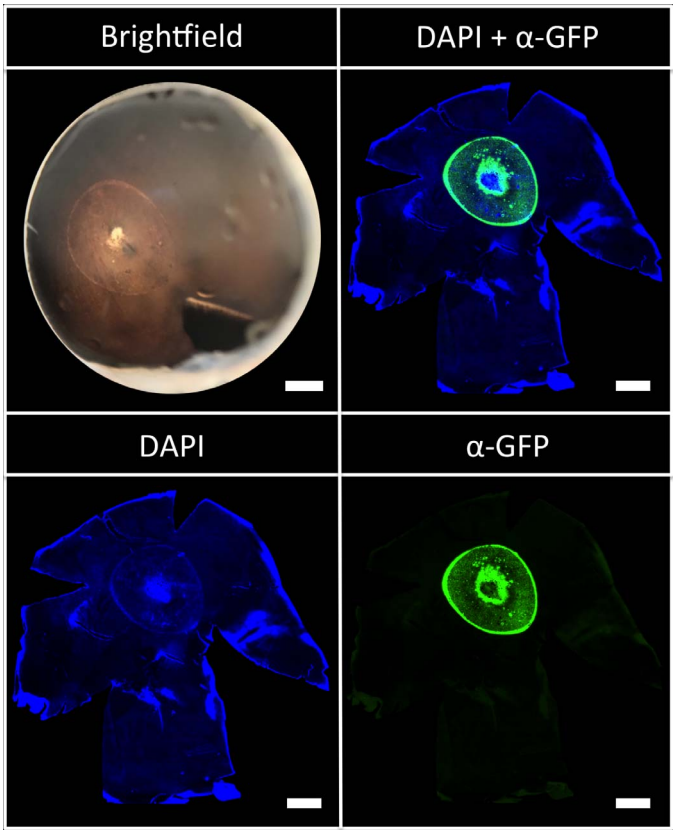

Figure 4. Transduction within subretinal bleb following subretinal injection of A3V. Whole-mounted chick retina 21 days after subretinal injection of EGFP-encoding A3V. Scale bar = 2 mm.

transduced cells, retinal ganglion cell axons in the nerve fiber layer were observed as striations just beneath the vitreal surface of the retinal whole mounts. As can be inferred from the whole-mount image, representative cross sections of these retinas featured few, if any, transduced neurons and, thus, were not included. Although this low efficiency of cell transduction is not ideal for experimental manipulations of gene expression, it does allow for in situ visualization and three-dimensional reconstruction of retinal cells with complex morphologies (see Figs. 8C, 8F, 8G). Although outside of the aims of this research project, this may prove valuable in identifying and characterizing cells of the avian retina that have not yet been visualized by other methods.[33–35]

Transduction of the Retina following Subretinal Injection

Although intravitreal injection of EGFP-encoding A3V vectors yielded infrequent transduction of cells deep to the inner limiting membrane (ILM), throughout the retina (Fig. 3), subretinal injection of these vectors resulted in highly efficient transduction of retinal cells bordering the subretinal space. The site of the subretinal injection and resulting "bleb" were visualized via bright-field microscopy and fluorescence microscopy of DAPI-labeled nuclei. As can be seen in Figure 4, intense EGFP expression was observed, entirely localized to the subretinal bleb. Although this labeling was apparently most concentrated in concentric rings around the outside of the bleb and injection site, subsequent visualization of additional subretinal-injections and retinal cross sections proved this to be due to variable blocking of light by adherent RPE cells, rather than to variable expression within the bleb (See Fig. 6). It should be noted that attempts to reproduce these results in broiler chick retinas were largely unsuccessful, suggesting that transduction efficiency may be strain-specific (data not shown).

Given that a successful subretinal injection delivers solution between the retina and RPE, one would expect the RPE to exhibit a similar pattern of EGFP expression if RPE cells are susceptible to transduction by recombinant A3V. Indeed, visualization of whole-mounted RPE revealed strong EGFP expression in

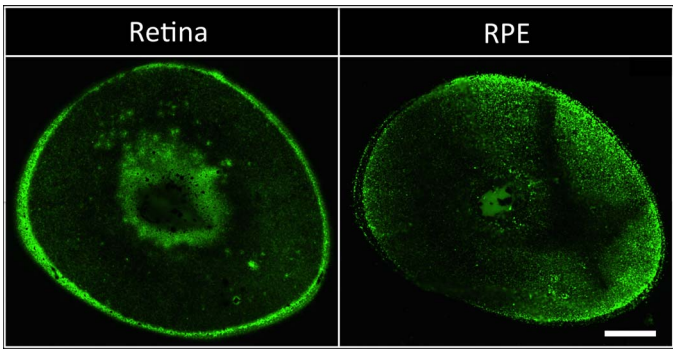

Figure 5. Transduction of both retina and RPE following subretinal injection of A3V. Comparison of EGFP expression in subretinal "bleb" region of retinal and RPE wholemounts 21 days following subretinal delivery of EGFP-encoding A3V. Scale bar = 1 mm.

RPE cells completely localized to the subretinal bleb (Fig. 5).

Highly Efficient Transduction of Photoreceptors with Subretinal Delivery

To determine the selective cell tropism of transduction following subretinal injection with EGFP-encoding A3Vs, retinal cross sections from subretinally injected chick eyes were analyzed. Given the damaging nature of the subretinal injection, it is not surprising that some retinal dystrophy and degeneration could be observed near the site of injection, as previously reported.[24] These regions were avoided during sectioning when possible. The most striking observation in these retinas was the frequency of finding strongly transduced photoreceptors within the subretinal bleb (See Fig. 6). Subjectively, all or nearly all photoreceptors were labeled within the majority of the undamaged region of the retinal bleb, with slightly less frequent transduction toward the bleb's periphery (Fig. 6B).

Photoreceptor transduction was analyzed in greater detail by using single confocal Z-slices of retinal cross sections (0.44 μm thickness). We observed transduction of rods, plus all types of cones (distinguishable by stratum of termination in the OPL, plus position of the soma in the ONL and general morphology; Fig. 7).[26] Once again, a comparison of EGFP expression and DAPI-labeled nuclei revealed that all or nearly all photoreceptors were transduced.

A3V is Capable of Transducing All Major Retinal Cell Types

Careful inspection of retinal whole mounts or cross sections revealed instances of EGFP expression in some cells of all other major retinal cell types, in addition to the highly efficient transduction of photoreceptors. Figure 8 shows representative examples of A3V-transduced RPE (A), photoreceptor (B), horizontal (C), amacrine (D), bipolar (E), Müller (F), and ganglion (G) cells. Transduction of oligodendrocytes—glial cells responsible for myelination of retinal ganglion cell axons, which is a normal feature of avian retinas[36]—was also occasionally observed in these retinas (data not shown).

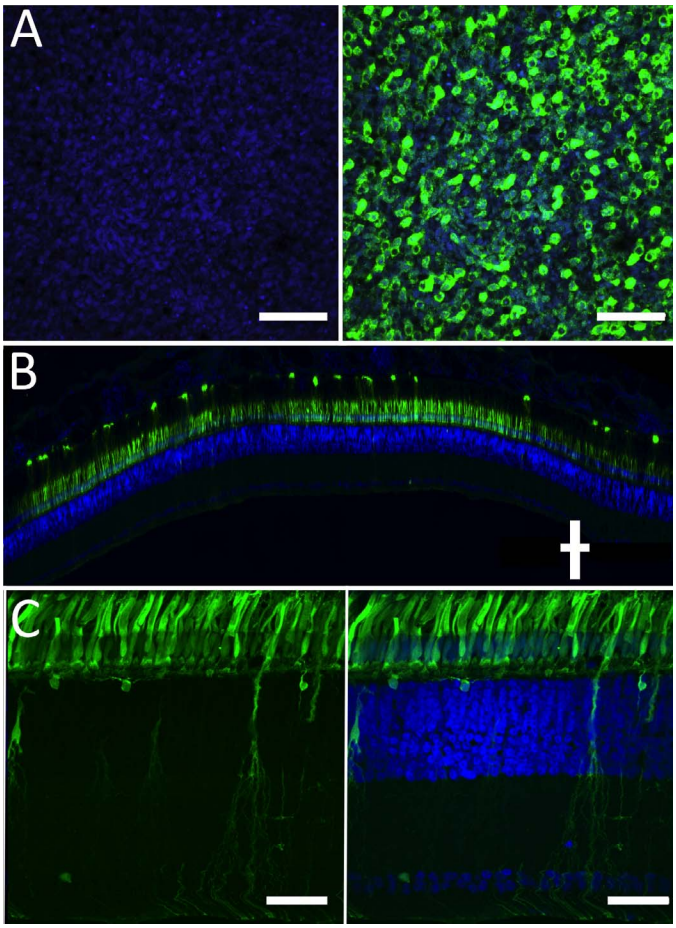

Figure 6. Retinal transduction of photoreceptors and other retinal cells following subretinal injection of A3V. (A) Whole-mounted chick retina (PR side up), prepared 14 days after subretinal injection of GFP-encoding A3V, showing DAPI (*Left*) and DAPI + anti-GFP (*Right*) labeling. Scale bar = 25 μm. (B) Retinal cross section of subretinal bleb 21 days after injection with EGFP-encoding A3V, labeled with DAPI and anti-GFP. Stretched vertically for better visualization of structure along transretinal axis. Scale bars = 100 μm. (C) Representative 60× retinal cross section of subretinal bleb 21 days after injection with EGFP-encoding A3V. Scale bar = 25 μm.

Various serotypes of AAV have been reported to exhibit different cell-specific tropisms in mammalian

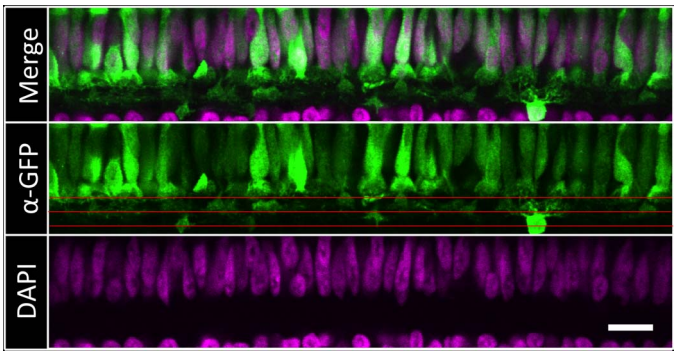

Figure 7. Photoreceptor transduction following subretinal injection of A3V. Confocal Z-slice (0.44 μm thick) of EGFP-encoding A3V transduced photoreceptors. Photoreceptors can be distinguished by morphology, position of soma within the ONL, and sublaminae of termination in the OPL (*middle image*, *red lines*) in which the axon terminates.[26] All types of photoreceptor are transduced and thus exhibit EGFP-expression. Scale bar = 10 μm.

retinas.[37] As the ability to transduce specific cells is directly relevant to the utility of A3V for experimental manipulation of gene expression, we quantified the apparent percent transduction of these different retinal cell types in cross sections of the transduced region of subretinally-injected retinas. Figure 9 represents the cumulative data for 22 imaged cross sections, from 8 separate retinas, performed with 3 separate EGFP-expressing A3V viral preparations. As can be seen, retinal cells other than rods and cones exhibit meagre transduction relative to their overall numbers, although substantially more frequent transduction is produced by subretinal than by intravitreal injection. Visual inspection of images revealed, surprisingly, that ganglion cells—found farthest from the subretinal space—were the most frequently transduced of all nonphotoreceptor cells. In contrast, bipolar and amacrine cells were transduced only rarely, whereas horizontal and Müller cells were more

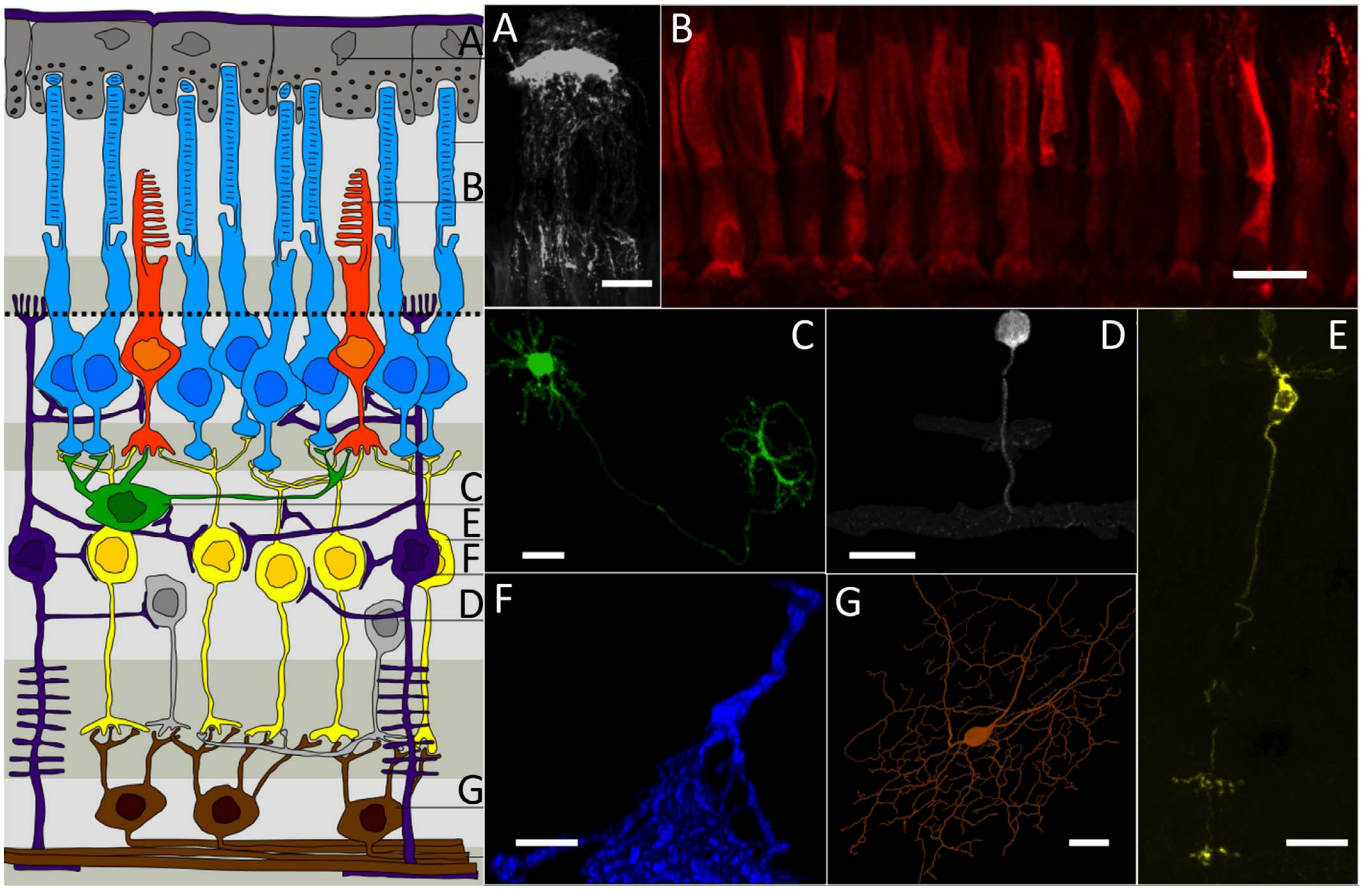

Figure 8. Transduction of all major subtypes of retinal cell with A3V. Representative examples of anti-EGFP immunolabeled A3V-CAG-EGFP transduced cells. RPE (A), photoreceptor (B), horizontal (C), amacrine (D), bipolar (E), Müller (F), and ganglion (G) cells are shown; pseudocolored to match the schematic retina shown in the *left panel*. The horizontal, Müller, and ganglion cells represent three-dimensional reconstructions from Z-stacks of images in intravitreally injected retinal whole-mounts. Scale bars = 10 μm for A–F, 25 μm for G.

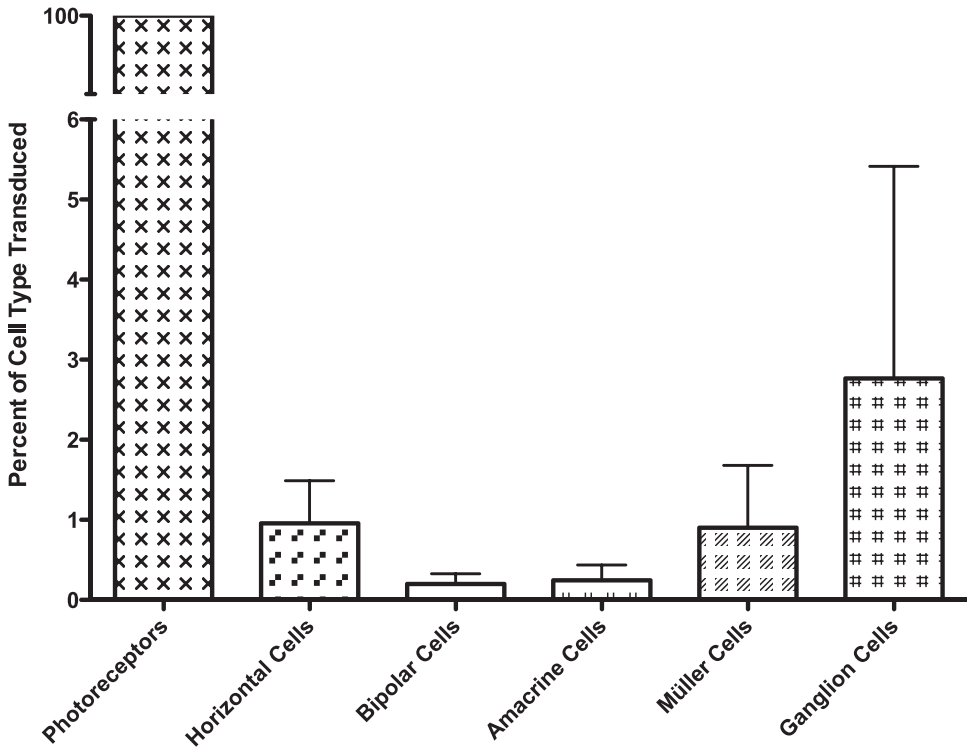

Figure 9. Quantification of cell-type transduction with A3V following subretinal injection. Frequency of transduction of cells within subretinal-injection blebs due to subretinal EGFP-encoding A3V delivery, relative to approximate total numbers of each cell type (Fig. 2; Table). The mean frequency of transduction was quantified from 22 sections, from 8 different subretinal injections, using 3 different EGFP-encoding A3V viral preps. Transduction rates measured within interior of subretinal bleb and do not include periphery or damaged regions resulting from injection.

frequently transduced but still less frequently than cells in the GCL.

Discussion

These experiments represent the first use of viral vectors to manipulate retinal gene expression in the postembryonic chick retina (to our knowledge)[3] and have established a promising avenue for future experiments in this valuable model. There are several caveats, however, and further optimization may broaden the utility of this experimental method.

The poor transduction observed with intravitreal injection is unfortunate, as intravitreal delivery is both technically easier and less invasive than subretinal injection, and can potentially mediate transduction within the entire horizontal extent of the retina (i.e., not limited to the subretinal bleb). Therefore, means to increase transduction with intravitreal delivery warrant further inquiry. Dalkara et al.[38] have shown that mild disruption of the ILM with the nonspecific protease Pronase E dramatically increased retinal transduction efficiency of AAV2 when delivered intravitreally in the mouse eye, without compromising visual function. Similarly, it has been shown that digestion of the glycosaminoglycans found in the mouse vitreous and on the surface of the ILM, with glycosidic enzymes, increases the transduction efficiency of intravitreally delivered AAV2.[39] Investigation into the glycosaminoglycans of the chick eye and research into the potential to disrupt these and the protein constituents of the chick eye without compromising retinal function may similarly enhance the depth and breadth of A3V transduction in the chick retina. It should be noted that the nerve fiber layer, which is located directly under the ILM, may pose an additional barrier to transduction after intravitreal delivery in the chick, as it differs from that of the mouse in being myelinated and substantially thicker.[40,41] The substantially larger vitreal volume of the chick globe, namely, ~40 fold that of the mouse,[42] may also hinder intravitreal transduction by diluting injected viral solution and, thus, reducing effective vector titer at retinal cells.[43] Higher titer A3V solutions and visually directed delivery into the liquid

layer of vitreous along the ILM might circumvent this issue.

The highly efficient transduction of chick rod and cone photoreceptors with subretinal injection does make A3V useful for many experimental aims, specifically those in which local gene expression or knock down is likely to produce a microscopically observable phenotype. For experiments in which measures of visual function are important, the fraction of the retina transduced is directly relevant. With our technique of delivering subretinal injections without visualization of the injection site, the portion of transduced retina was highly variable between experiments and it reached a maximum of only ~1/9th of the total retinal area. By contrast, detachment of approximately one-third of the retinal area has been reproducibly achieved by other investigators when the procedure is observed using a surgical microscope through a pharmacologically dilated pupil (unpublished observations).[24] A3V-mediated manipulation of relevant gene expression in photoreceptors of one-third of the retina is likely sufficient to produce measurable changes in behavioral and electrophysiological measures of visual function, expanding the potential uses of this technique. However, damage from both the subretinal injection and resulting retinal detachments also has deleterious effects on retinal function and morphology and might negatively affect these measurements during experimentation.[24]

The observation of differences in retinal transduction efficiency between Leghorn and broiler strains of chicken (data not shown) also may impose restrictions on future efforts to use A3V experimentally. Similar variability of transduction efficiency has been reported between strains of nude mice following intravenous AAV delivery.[44] As the few hereditary ocular diseases identified in chickens occur on specific genetic backgrounds (i.e., in specific strains), this serotype of A3V may not be able to transduce these retinal cells effectively in every case and, thus, may not be universally applicable to investigations or manipulations of retinal function in all chicken models.[3] As this phenomenon likely occurs in all species of laboratory animal, further investigations into the mechanisms underlying this strain-specific transduction are warranted.

Finally, the highly efficient transduction of rods and cones by subretinally delivered A3V, compared to that of other retinal neurons, suggests that photoreceptors might be particularly susceptible to A3V transduction. Retinal cell type-specific tropism has also been reported in other AAV serotypes and is likely a result of differences in receptor binding due to variations in viral capsid structure.[45] The cell-surface receptor/binding determinant recognized by A3V has yet to be determined, and its eventual discovery may explain this observed tropism and provide mechanisms to increase transduction efficiency (by digesting competing binding sites in the vitreous or barriers in the ILM, for example). Alternatively, manipulation of the A3V capsid protein may increase tropism for nonphotoreceptor cells and may even increase transduction following intravitreal injection. Significant changes in tropism and transduction efficiency of mouse retina have been achieved with AAV2 virions, by in vivo-directed evolution.[15,32] We suggest that similar efforts using the A3V capsid may provide similar results in the chicken retina, increasing both the potential power of this animal model and the utility of this vector.

The use of A3V as opposed to other AAV vectors in this study was based on observations made by Matsui et al.,[18] which showed significantly more transduction of postembryonic chicken neurons with A3V compared to AAV2 and lentivirus. This does not, however, mean that A3V is the optimal vector for transduction of the chicken retina, and other vectors may result in more efficacious transduction. In particular, recently created recombinant AAVs have shown highly efficient transduction of retinal cells in mammalian models and may show similar efficacy in the postembryonic chicken.[46–48] Although outside the scope of this study, further investigation into the transduction efficiency of other AAV vectors in this model may be incredibly valuable.

In conclusion, we have described a novel, efficient method for manipulation of gene expression in photoreceptors of the postembryonic chicken retina. Further research can be expected to produce dramatic increases in the utility of this vector for experimental studies. Even without further improvements, however, this approach has excellent potential for cell type-specific modification of gene expression, which should be useful for investigating many aspects of retinal circuitry and function in this powerful model.

Acknowledgments

The authors thank Ryosuke Matsui and Dai Watanabe (Kyoto University, Kyoto, Japan) for the gift of A3V plasmids, Jay Chiorini (National Institute of Health, National Institute of Dental and Cranio-

facial Research) for helpful advice and plasmids, and Brittany Carr (Department of Ophthalmology, University of British Columbia) for assistance and support of many kinds.

Supported by grants from the Foundation Fighting Blindness-Canada (FFB-EyeGeye Research Training Fund to WKS; studentship to DMW), Natural Sciences and Engineering Research Council (Discovery Grant RGPIN/131-2013 to WKS), and the University of Calgary (Lions Sight Centre Fund to NTB-H and WKS). Microscopy facilities were provided by the Live Cell Imaging Facility, funded by the Snyder Institute, at the Cumming School of Medicine, University of Calgary.

Disclosure: **D.M. Waldner**, None; **F. Visser**, None; **A.J. Fischer**, None; **N.T. Bech-Hansen**, None; **W.K. Stell**, None

References

1. Perlman RL. Mouse models of human disease: an evolutionary perspective. *Evol Med Public Health*. 2016;2016:170–176.
2. Huberman AD, Niell CM. What can mice tell us about how vision works? *Trends Neurosci*. 2011; 34:464–473.
3. Wisely CE, Sayed JA, Tamez H, et al. The chick eye in vision research: an excellent model for the study of ocular disease. *Prog Retin Eye Res*. 2017; 61:72–97.
4. Doyle A, McGarry MP, Lee NA, Lee JJ. The construction of transgenic and gene knockout/ knockin mouse models of human disease. *Transgenic Res*. 2012;21:327–349.
5. Dean S. Transgenic animal mutation models: a review of the models and how they function. *Methods Mol Biol*. 2012;817:377–397.
6. Kurian KM, Watson CJ, Wyllie AH. Retroviral vectors. *Mol Pathol*. 2000;53:173–176.
7. Williams ML, Coleman JE, Haire SE, et al. Lentiviral expression of retinal guanylate cyclase-1 (RetGC1) restores vision in an avian model of childhood blindness. *PLoS Med*. 2006;3:e201.
8. Verrier JD, Madorsky I, Coggin WE, et al. Bicistronic lentiviruses containing a viral 2A cleavage sequence reliably co-express two proteins and restore vision to an animal model of LCA1. *PLoS One*. 2011;6:e20553.
9. Vergara MN, Canto-Soler MV. Rediscovering the chick embryo as a model to study retinal development. *Neural Dev*. 2012;7:22.
10. Harpavat S, Cepko CL. RCAS-RNAi: a loss-of-function method for the developing chick retina. *BMC Dev Biol*. 2006;6:2–2.
11. Fischer AJ, Stanke JJ, Omar G, Askwith CC, Burry RW. Ultrasound-mediated gene transfer into neuronal cells. *J Biotechnol*. 2006;122:393–411.
12. Zinn E, Vandenberghe LH. Adeno-associated virus: fit to serve. *Curr Opin Virol*. 2014;8:90–97.
13. Hanna E, Rémuzat C, Auquier P, Toumi M. Gene therapies development: slow progress and promising prospect. *J Mark Access Health Policy*. 2017;5:1265293.
14. Srivastava A. In vivo tissue-tropism of adeno-associated viral vectors. *Curr Opin Virol*. 2016;21: 75–80.
15. Reid CA, Ertel KJ, Lipinski DM. Improvement of photoreceptor targeting via intravitreal delivery in mouse and human retina using combinatory rAAV2 capsid mutant vectors. *Invest Ophthalmol Vis Sci*. 2017;58:6429–6439.
16. Bossis I, Chiorini JA. Cloning of an avian adeno-associated virus (AAAV) and generation of recombinant AAAV particles. *J Virol*. 2003;77: 6799–6810.
17. Yates VJ, el-Mishad AM, McCormick KJ, Trentin JJ. Isolation and characterization of an Avian adenovirus-associated virus. *Infect Immun*. 1973;7:973–980.
18. Matsui R, Tanabe Y, Watanabe D. Avian adeno-associated virus vector efficiently transduces neurons in the embryonic and post-embryonic chicken brain. *PLoS One*. 2012;7:e48730.
19. Waldner DM, Visser F, Stell WK. An avian adeno-associated viral vector for visualization of post-natal chick retinal circuitry. *Invest Ophthalmol Vis Sci* 2017;58:5905.
20. Zolotukhin S, Byrne BJ, Mason E, et al. Recombinant adeno-associated virus purification using novel methods improves infectious titer and yield. *Gene Ther*. 1999;6:973–985.
21. Reid CA, Lipinski DM. Small and micro-scale recombinant adeno-associated virus production and purification for ocular gene therapy applications. *Methods Mol Biol* 2018;1715:19–31.
22. Matsuda T, Cepko CL. Electroporation and RNA interference in the rodent retina in vivo and in vitro. *Proc Natl Acad Sci U S A*. 2004;101:16–22.
23. Carr BJ, Stell WK. Nitric Oxide (NO) Mediates the inhibition of form-deprivation myopia by atropine in chicks. *Sci Rep*. 2016;6:9.

24. Cebulla CM, Zelinka CP, Scott MA, et al. A chick model of retinal detachment: cone rich and novel. *PLoS One*. 2012;7:e44257.
25. Bueno JM, Giakoumaki A, Gualda EJ, Schaeffel F, Artal P. Analysis of the chicken retina with an adaptive optics multiphoton microscope. *Biomed Opt Express* 2011;2:1637–1648.
26. López-López R, López-Gallardo M, Pérez-Álvarez MJ, Prada C. Isolation of chick retina cones and study of their diversity based on oil droplet colour and nucleus position. *Cell Tissue Res*. 2008;332:13–24.
27. Boije H, Shirazi Fard S, Edqvist P-H, Hallböök F. Horizontal cells, the odd ones out in the retina, give insights into development and disease. *Front Neuroanat*. 2016;10:77.
28. Gallina D, Zelinka C, Fischer AJ. Glucocorticoid receptors in the retina, Muller glia and the formation of Muller glia-derived progenitors. *Development*. 2014;141:3340–3351.
29. Stanke JJ, Lehman B, Fischer AJ. Muscarinic signaling influences the patterning and phenotype of cholinergic amacrine cells in the developing chick retina. *BMC Dev Biol*. 2008;8:13.
30. Kalloniatis M, Tomisich G, Marc RE. Neurochemical signatures revealed by glutamine labeling in the chicken retina. *Vis Neurosci*. 1994;11:793–804.
31. Kalloniatis M, Napper GA. Glutamate metabolic pathways in displaced ganglion cells of the chicken retina. *J Comp Neurol*. 1996;367:518–536.
32. Dalkara D, Byrne LC, Klimczak RR, et al. In vivo-directed evolution of a new adeno-associated virus for therapeutic outer retinal gene delivery from the vitreous. *Sci Transl Med*. 2013; 5: 189ra176.
33. Fischer AJ, Stanke JJ, Aloisio G, Hoy H, Stell WK. Heterogeneity of horizontal cells in the chicken retina. *J Comp Neurol*. 2007;500:1154–1171.
34. Gardino PF, de-Oliveira MM, de-Gamboa RM, Hokoc JN. Two novel types of bistratified amacrine cells in the chick retina: a Golgi study. *Braz J Med Biol Res*. 1994;27:1639–1646.
35. Quesada A, Prada FA, Genis-Galvez JM. Bipolar cells in the chicken retina. *J Morphol*. 1988;197:337–351.
36. Nakazawa T, Tachi S, Aikawa E, Ihnuma M. Formation of the myelinated nerve fiber layer in the chicken retina. *Glia* 1993;8:114–121.
37. Hellström M, Ruitenberg MJ, Pollett MA, et al. Cellular tropism and transduction properties of seven adeno-associated viral vector serotypes in adult retina after intravitreal injection. *Gene Ther*. 2008;16:521.
38. Dalkara D, Kolstad KD, Caporale N, et al. Inner limiting membrane barriers to AAV-mediated retinal transduction from the vitreous. *Mol Ther*. 2009;17:2096–2102.
39. Cehajic-Kapetanovic J, Le Goff MM, Allen A, Lucas RJ, Bishop PN. Glycosidic enzymes enhance retinal transduction following intravitreal delivery of AAV2. *Mol Vis*. 2011;17:1771–1783.
40. Imagawa T, Fujita Y, Kitagawa H, Uehara M. Quantitative studies of the optic nerve fiber layer in the chicken retina. *J Vet Med Sci*. 1999;61:883–889.
41. Ferguson LR, Dominguez JM, Ii Balaiya S, Grover S, Chalam KV. Retinal thickness normative data in wild-type mice using customized miniature SD-OCT. *PLoS One*. 2013;8:e67265.
42. Pickett-Seltner RL, Doughty MJ, Pasternak JJ, Sivak JG. Proteins of the vitreous humor during experimentally induced myopia. *Invest Ophthalmol Vis Sci*. 1992;33:3424–3429.
43. Kaplan HJ, Chiang CW, Chen J, Song SK. Vitreous volume of the mouse measured by quantitative high-resolution MRI. *Invest Ophthalmol Vis Sci*. 2010;51:4414–4414.
44. Colbern GT, Luan B, Tu GH, et al. 375. Transduction efficiency of nude mice with aav vectors for gene transfer: effect of mouse strain or vendor. *Mol Ther*. 2003;7:S147.
45. Castle MJ, Turunen HT, Vandenberghe LH, Wolfe JH. Controlling AAV tropism in the nervous system with natural and engineered capsids. *Methods Mol Biol*. 2016;1382:133–149.
46. Katada Y, Kobayashi K, Tsubota K, Kurihara T. Evaluation of AAV-DJ vector for retinal gene therapy. *PeerJ* 2019;7:e6317.
47. Hickey DG, Edwards TL, Barnard AR, et al. Tropism of engineered and evolved recombinant AAV serotypes in the rd1 mouse and ex vivo primate retina. *Gene Ther*. 2017;24:787–800.
48. Boye SE, Alexander JJ, Witherspoon CD, et al. Highly efficient delivery of adeno-associated viral vectors to the primate retina. *Hum Gene Ther*. 2016;27:580–597.